(Received 24 September 2024, Accepted 2 December 2024, Scheduled 14 December 2024)

A Compact Monopole Slotted Patch-Antenna for UWB Applications

Yousif Mohsin Hasan*

Department of Electronic and Communication Engineering, College of Engineering, University of Al-Qadisiyah, Iraq

ABSTRACT: This paper presents a compact single-feed, rectangular slotted-patched antenna (SPA) for UWB applications. The proposed design adds a triangular part of the tail of the rectangular patch, cuts the edge of the patch, etches a rectangular slot in the ground plane, and then tunes the basic parameters of the design to achieve the UWB passband. The proposed antenna including slots on the patch for compact functionality is readily identifiable. The bandwidth and realized gain of the UWB antenna can be extremely improved to show the ability of a slot loading technique. The new conception of the rectangular patch antenna is considered. A feed mechanism using an inset patch feedline is implemented and analyzed. The parameters of the antenna are demonstrated, and the antenna is fabricated with an inexpensive FR4 substrate and validated experimentally. The antenna occupies frequency band (2.56–12) GHz. Making slots in the modified patch results in a significant gain improvement of 4.8 dBi as well as extending the UWB passband. The measured values of the reflection coefficient, VSWR, realized gain, and power pattern are in good agreement with the simulated results.

1. INTRODUCTION

Patch antennas have numerous advantages in terms of compression compared to conventional antennas. A patch antenna is a compact radiating device that can be assembled specifically for some applications. These devices are low cost, compressed, not bulky, conformable, and flexible in frequency [1]. The Federal Communication Commission (FCC) has approved commercial ultra-wideband (UWB) operations ranging from 3.1 to 10.6 GHz. This technology has piqued the interest of researchers [2, 3]. UWB technology now allows for high data rate transmission with minimal latency and power consumption [4, 5] and has attracted the attention of both academics and industry over the past two decades. This technology has various uses, from wireless sensor networks to biomedical imaging and is not just restricted to satellite communication or military uses [6–8]. An antenna's UWB passband is obtained by truncating the bottom ends of a rectangular patch antenna [9]. The impedance bandwidth of 3–14.55 GHz is achieved by the rectangular antenna proposed by [10]. There are numerous applications for UWB in modern wireless communication. Antennas with rectangular patches are usually considered $\lambda/2$ antennas [11]. A staircase patch structure is used to improve the bandwidth by decreasing the capacitance between the ground plane and the patch [12]. The proposed antennas by [13–15] have a large size, and they do not cover the standard UWB spectrum. The antenna proposed by [16] has dual bandwidths, the first being (3.65–7.49) GHz and the second being (11.5–13.4) GHz. Planar Inverted-L patch is a desirable choice for UWB [17]. Embedding appropriate slots in the ground plane or the radiating patch of the antenna shall result in a compact antenna, which can be utilized for UWB applications [18]. The rectangular patch with an L-shaped incision can reach an improved operating frequency of 2.45 GHz (the Industrial Scientific Medical band) [19]. Moving the feed point near or far from the grounded edge will locate the 50-ohm point. The impedance should increase as the feed moves away from the ground edge [20].

In this paper, an enhanced antenna gain and a wider impedance bandwidth are discussed. When the proposed antenna is used, the increase in resonant frequency leads to a possible reduction in the size of the antenna. All of these merits are considered advantages over compact designs with a slotted radiating patch. For indoor wireless communication applications, such merits are considered advantageous. This shows that, in addition to its low cost of construction, the proposed antenna is also convenient for mobile stations and UWB applications. This work can be divided into sections. In Section 2, steps to modify a rectangular UWB antenna are introduced along with the necessary design steps. The antenna parametric study of the proposed antenna is discussed in Section 3. The results of the proposed antenna are discussed in Section 4. The conclusion extracted from this work is presented in Section 5.

2. STEPS TO MODIFY A RECTANGULAR UWB ANTENNA

The rectangle-shaped $\lambda/2$ monopole antenna was initially designed with Computer Simulation Technology (CST). This design is a modified version of the antenna presented in [21], which is a rectangular planar monopole UWB antenna. A UWB antenna based on a dielectric substrate of dimensions $(W_s \times L_s = 34 \times 38)$ mm^2 is firstly designed at an operating fre-

* Corresponding author: Yousif Mohsin Hasan (yousif.hasan@qu.edu.iq).

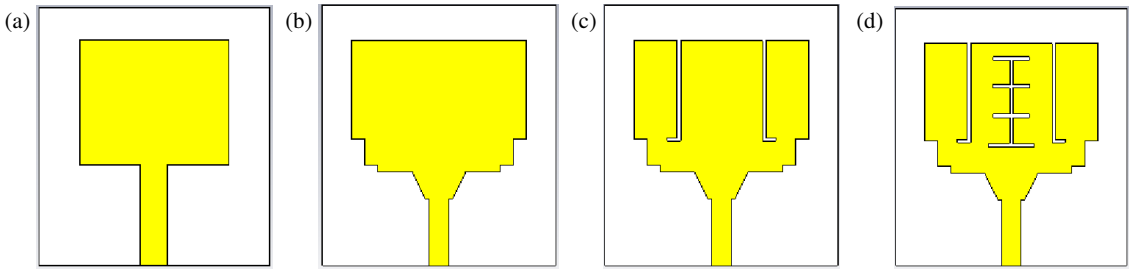

FIGURE 1. Steps to develop proposed antenna, (a) Step1, (b) Step2 (c) Step3, (d) Step4.

quency of 3.1 GHz, aiming for compact size at the lowest band of the UWB. An inexpensive FR4 substrate was used in this design with dielectric permittivity $\epsilon_r = 4.3$, height $h = 1.4$ mm, and loss tangent $\tan\delta = 0.025$. The patch feed-line is a 50 Ω strip line that has two sided slant edges. The width (W_f) of the feed line was calculated to be 2.4 mm to achieve impedance matching. The antenna provides a partial ground plane for the broadband impedance matching [21, 22]. The radiating patch dimensions were ($W \times L = 29.7 \times 24.2$) mm^2 , and they are found according to the transmission line model basic equations [23]. The rectangular patch with steps designed to develop the proposed antenna is presented in Figure 1. A patch antenna loaded with slots for compact operation is easily recognized. The bandwidth of the UWB antenna can be greatly improved to show the ability of a slot loading technique. The new conception of the rectangular patch antenna is considered. A feed mechanism using an inset patch feed-line is implemented and analyzed. The initial dimension of the patch antenna can be calculated using the following equations [23–25].

$$W = \frac{c}{2f \times \sqrt{\frac{\epsilon_r+1}{2}}} \tag{1}$$

$$\epsilon_{eff} = \frac{\epsilon_r + 1}{2} + \frac{\epsilon_r - 1}{2}\left[1 + \frac{12h}{W}\right]^{-0.5} \tag{2}$$

$$L = \frac{c}{2f \times \sqrt{\epsilon_{eff}}} \tag{3}$$

where W, L, f, c, ϵ_r, ϵ_{eff}, and h are the width of the patch antenna, length of the patch antenna, resonant frequency, speed of light in free space, dielectric constant, effective dielectric constant, and height of substrate, respectively.

The reflection coefficient of the initial antenna is simulated by CST as shown in Figure 2 which is bad matching. At first, the reduction in antenna gain resulting from the loss of the transmission line slope edges must be considered for practical applications. Such a reduction is approximately 2 dBi. Furthermore, the large loss tangent is considered the main reason for the lower antenna gain (typically 0.025), and it is related to the FR4 substrates used.

To improve the proposed antenna's gain, different slots with different lengths are presented in the patch. A staircase patch structure and a band-notch in the ground plane are both attached to enhance the capacitive coupling between the ground plane

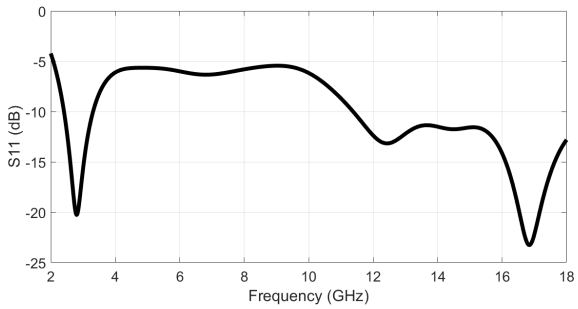

FIGURE 2. The reflection coefficient of the antenna with initial parameter.

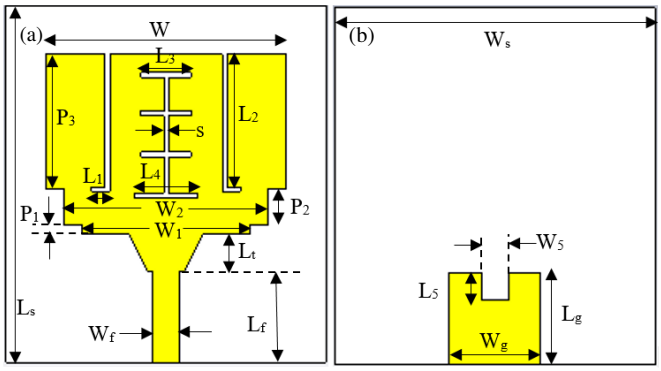

FIGURE 3. Modified slotted antenna, (a) patch, (b) ground plane.

and the patch, which usually results in a wider impedance bandwidth [26]. The modified design is shown in Figure 3, and all the parameter values are listed in Table 1.

3. ANTENNA PARAMETRIC STUDY

All the parameters in a rectangular patch antenna (L, W, h, permittivity dimensions of the ground plane, feed width size, feed point position) are designed to control the antenna properties. This paper presents a reassessment of how these factors impact the antenna's performance, in order to present a design process that improves the antenna's response.

3.1. Modifying the Length of Patch

When there are no inserted slits, increasing the patch length leads to shifting the patch's dominant mode slightly to lower frequencies. Figure 4 shows that the obtained bandwidth is

TABLE 1. Parameter values of the modified rectangular antenna.

Parameter	W_s	W	W_f	s	W_5	W_g	L_5	L_g	P_1	P_2
Values (mm)	22	18	2.4	0.5	2	15	3	12	1	2.5
Parameter	L_s	P_3	L_f	L_1	L_2	L_3	L_4	L_t	W_1	W_2
Values (mm)	35	14.5	12	1.8	14.4	6	7	3.5	16	17

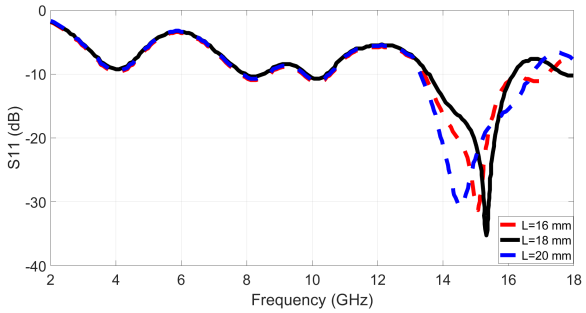

FIGURE 4. Reflection coefficient for different L.

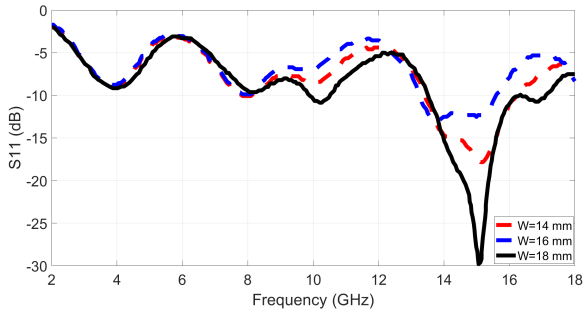

FIGURE 5. Reflection coefficient for different W.

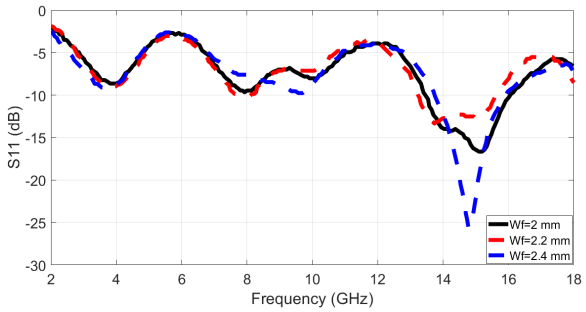

FIGURE 6. Reflection coefficient for different W_f.

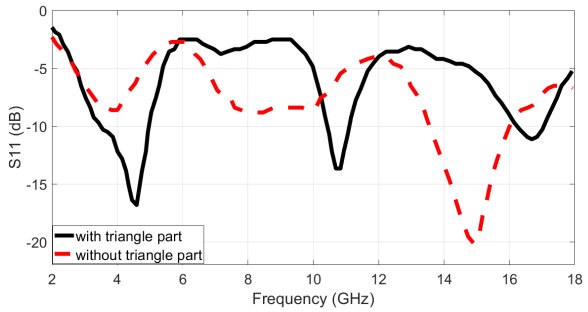

FIGURE 7. Reflection coefficient for with and without triangular part.

about 1.4%, which is largely dependent on the effective length of this patch.

3.2. Modifying the Width of Patch

The simulation S-parameter in Figure 5 shows that the decrease in patch width results in lowering the quality factor of the patch antenna and hence enhancing the impedance bandwidth.

3.3. Effect of Feeder Width

A structure of feeding that uses a 50-ohm transmission line with two-sided slant edges was investigated herein with a feed length of 9 mm. This has resulted in obtaining good matching conditions and achieving a wide impedance bandwidth. Figure 6 shows that the resonance frequency is 14.7 GHz and that the bandwidth is 9.8%. This is largely due to the slant edges of the feed line, which reduces the effective length of the current surface of the excited patch. However, at lower bands, it can be seen that the impedance matching is getting worse. Also, the impedance matching increases when the feeder width is near $\lambda/40$ [27, 28], and thus a larger bandwidth is obtained. Figure 4 shows that the resonance frequency is 14.7 GHz and that the bandwidth is 9.8%.

3.4. Effect of Adding Triangular Part of the Patch

The presentation of the triangular shape attached to the bottom of the patch will enhances the matching impedance. The optimal dimension of the modified triangular shape in the constructed prototype is determined by experiment. In addition to shifting the original resonance band from 15.6 GHz to 16.8, Figure 7 shows that the proposed arrangement produces two more resonance bands at 4.8 GHz and 10.8 GHz.

3.5. Effect of Ground Plane Width

By tuning the coupling slot diminutions and the width of the patch feed line, the proposed patch can be effectively matched to the electromagnetic energy of the patch feed line printed on the other side of the ground substrate, as shown in Figure 8.

3.6. Slotted Ground Plane Usage

A band-notch is etched in the ground plane to implement a capacitive coupled ground structure (see Figure 9). Since the band-notch modifies the distance between the lowest edge of the patch and the partial ground, the capacitive coupling between the patch and ground plane is also modified, which results in a wider impedance bandwidth. This notch is located

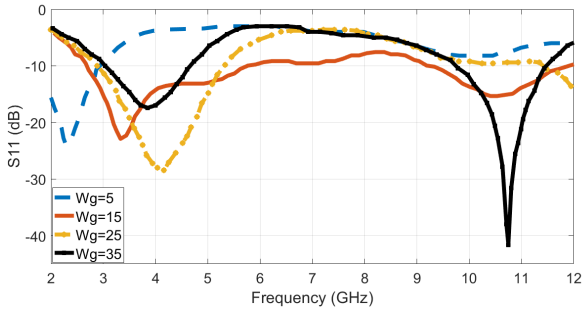

FIGURE 8. Reflection coefficient for different W_g.

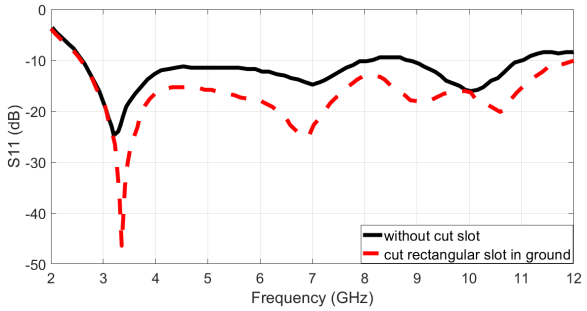

FIGURE 9. Reflection coefficient for adding slot in ground plane.

near the feeding point to provide additional electromagnetic coupling. The center frequency of the band notch (f_{notch}) can be predicted using the formula in [29].

3.7. Modified Shape and Right Angle Slots

Figure 10 illustrates the improvement in bandwidth for a rectangular patch antenna by using a promising slot loading design. In the design, two right-angle slots are located close to the non-radiating edges. Also, the width of the two right-angle slots is referred to as w_{s1}. The length of the shorter arm of the slots is referred to as L_1 and is about 10% of the patch length, and the shorter slot is perpendicular to the non-radiating edges. The length of the longer arm of the slots is referred to as L_2, and it is about 80% of the patch length. Also, the non-radiating edges and the longer arm are usually designed parallel to each other. Generally, experimental procedures are used to determine the length of the longer and shorter arms of the slots (L_1 and L_2). Although it is possible to achieve two operating frequencies using only right-angle slots, they are insufficient to create a single wide operating bandwidth. Regardless, a wide impedance bandwidth is still possible. This can be achieved by planting a slot with a modified shape along the center line of the patch. Such measures are expected to lower the frequency of the first resonance f_1 while keeping the other frequency f_2 almost unaffected. The width of the modified shape slot is referred to as w_{s1}. Furthermore, it has upper and lower sections of lengths L_3 and L_4, respectively. The integrated reactive loading is formed by four parallel slots joined by one perpendicular slot. It is introduced at the patch's center. The main design

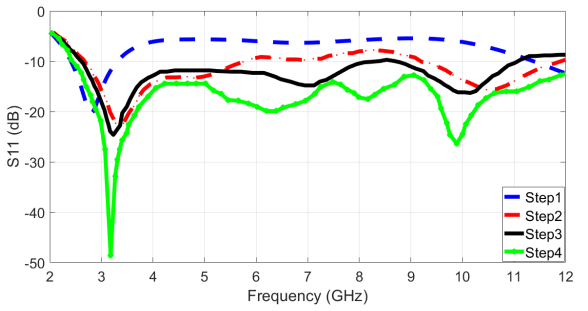

FIGURE 10. Reflection coefficient for steps of antenna modification and adding slots in the patch.

purpose of the modified shape slot is to further decrease the first frequency by perturbing the excited patch surface current path. Furthermore, good impedance matching can be achieved for both frequencies when using the modified shape slot. An experimental procedure was used to determine the convenient dimensions of the modified shape slot, which are as follows; upper section $L_3 = 6\,\text{mm}$, lower section $L_4 = 7\,\text{mm}$, and width $w_{s1} = 0.5\,\text{mm}$. The impedance bandwidth obtained is much wider than that of the regular rectangular patch antenna. Also, a size reduction of the proposed antenna was received from the targeted operating frequency band. The resonant mode occurred at a lower resonant frequency.

4. MEASUREMENT AND SIMULATION RESULTS

The performance of the design is practically verified by fabricating the modified antenna, as shown in Figure 11. Measurements have been made at the Ministry of Science and Technology in Baghdad using the Vector Network Analyzer. The input impedance, reflection coefficients (S_{11}), and voltage standing wave ratio (VSWR) were measured using a vector network analyzer (VNA) Anritsu-MS4642A (20 GHz) package. Figure 12 illustrates the relationship between the frequency and the simulated (with and without slots) and measured antenna gains. Based on the figure, a peak antenna gain of 4.8 dBi was achieved. Through adding slots in the patch antenna, the directivity and reflection coefficient are improved, which thus leads to improving the realized gain of the antenna. This shows that, in addition to its low cost of construction, the proposed antenna

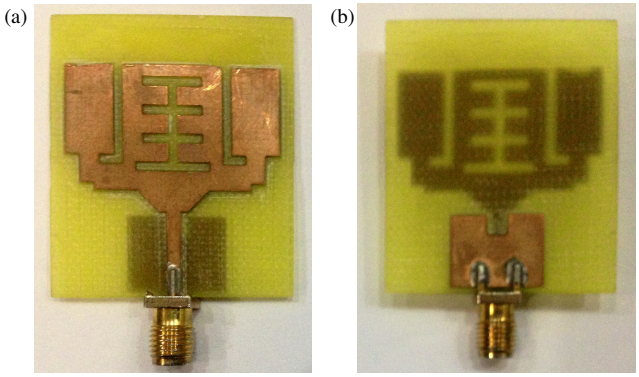

FIGURE 11. Fabricated proposed antenna, (a) patch, (b) ground plane.

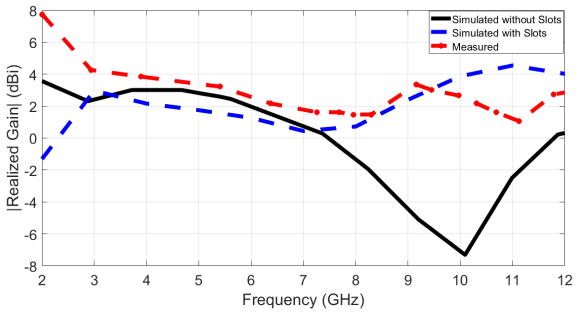

FIGURE 12. Simulated and measured gains of the proposed antenna.

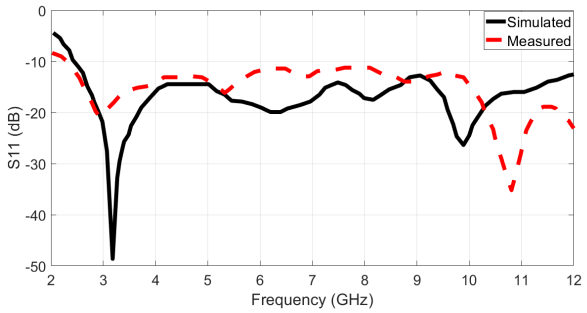

FIGURE 13. Simulated and measured reflection coefficients for the proposed antenna.

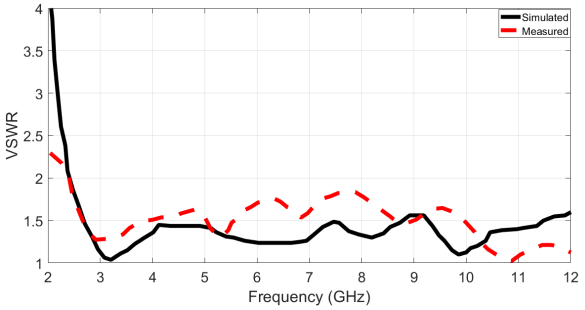

FIGURE 14. Simulated and measured VSWRs for the proposed antenna.

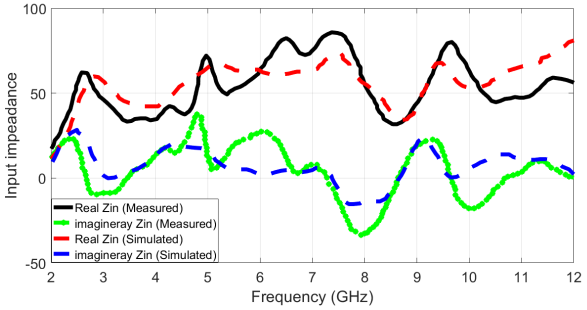

FIGURE 15. Simulated and measured input impedances of the proposed antenna.

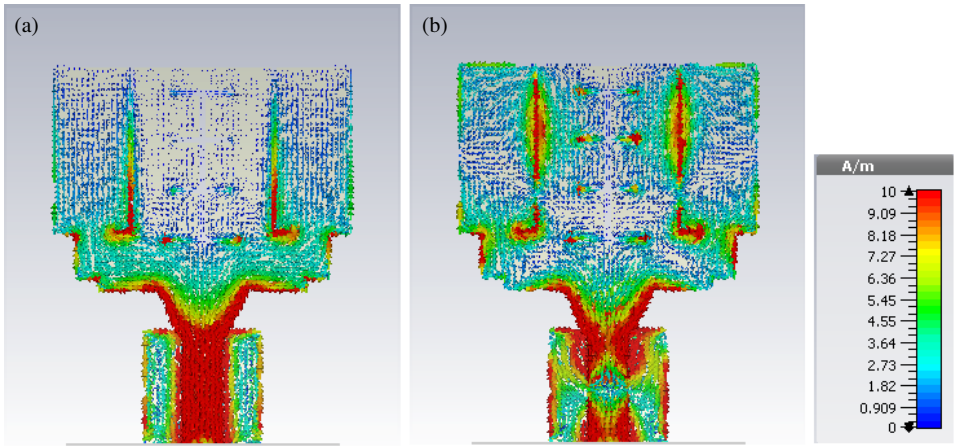

FIGURE 16. Current distribution at different frequency, (a) $f = 3.4$ GHz, (b) $f = 10$ GHz.

is also convenient for mobile stations and UWB applications. Figure 13 illustrates the simulated and measured reflection coefficients S_{11} of the proposed antenna along the UWB passband. Figure 14 shows the simulated and measured VSWRs of the proposed antenna and shows that they are less than 2 along the UWB passband. The comparison of the simulated and measured input impedances of the proposed antenna is shown in Figure 15.

Also, it is firmly established that the embedded slots strongly affect the excited surface currents in the radiating patch. As a result, the equivalent surface current increases. This generally leads to reducing the central frequency of the antenna, which coincides with the results obtained from measurements. Also, an increase was observed in total excited patch surface currents. Furthermore, an increase was also observed in the excited surface current distribution in the central portion of the radiating patch as shown in Figure 16. Figure 17 illustrates the simulated (measured) radiation patterns of the proposed antenna in the H-plane and E-plane at the frequencies of 3.4 GHz and 10 GHz. The radiation power pattern is calibrated depending on the gain of the antenna. The H-plane shows omnidirectional radiation power patterns at all three frequencies, meaning that the antenna radiates in all directions. On the other hand, in the E-plane, the antenna has bidirectional radiation patterns. The comparison of the proposed antenna with others is listed in Table 2.

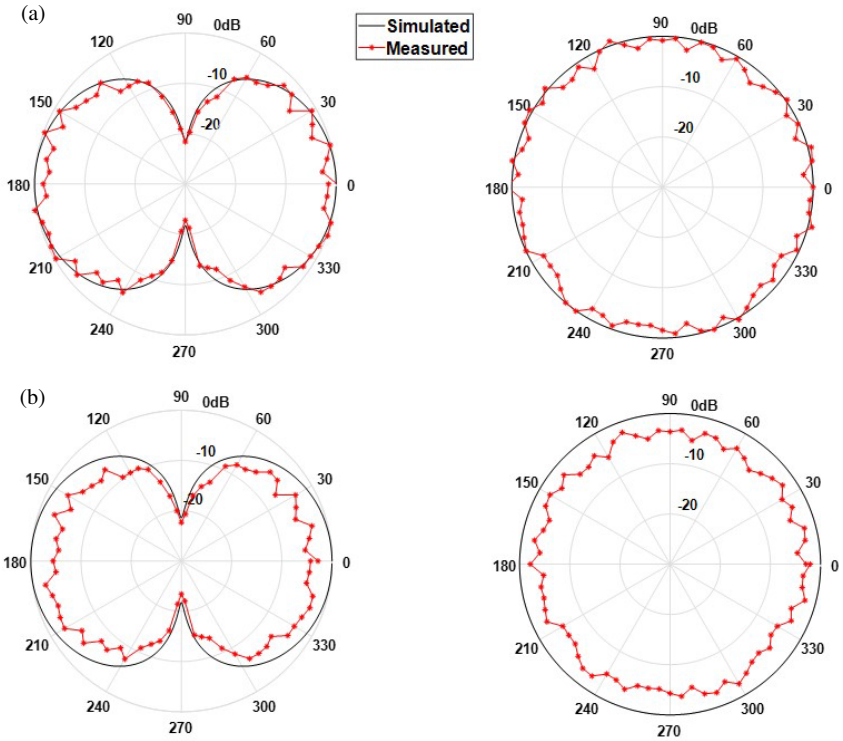

FIGURE 17. The radiation power patterns of the antenna at (a) 3.4 GHz, (b) 10 GHz.

TABLE 2. Comparison this work with other related works.

Reference No.	[9]	[30]	[31]	[32]	[33]	This work
Frequency (GHz)	7.7	3.54, 5.63	11	7.5	22	3.4, 10
Bandwidth (GHz)	3.1–12.5	3.3–3.78, 5.4–5.86	2.58–20.95	3–12	4–40	2.56–12
Gain (dBi)	4.5	3, 3.4	7.2	6.8	2.8	4.8
Size (mm)	16×25	50×50	26×22	72×72	28.1×17.1	22×35

5. CONCLUSIONS

A modified rectangular patch with various slots has been constructed. The UWB bandwidth requirements guided the design and analysis of the proposed antenna. Many enhancement techniques were used to achieve UWB bandwidth with improved antenna gain. The UWB bandwidth can be formed by the intersection of several narrowly distributed resonance bands, and the antenna that supports these bands can be considered a UWB antenna. The lower edge of the UWB characteristic of this antenna can be estimated by the dimensions of the patch. Varying the ground plane width shifts all the resonance frequencies of the spectrum, which affects the total width of the operating bandwidth. The bandwidth decreases when the ground plane width is too narrow or wide, and the bandwidth is reduced. It is found that the variation in ground plane length does not really change the bandwidth, because the current of the antenna is essentially spreading along the width direction. Therefore, the ground plane length can be reduced significantly without any sacrifice of bandwidth, which means that antenna miniaturization is possible. The impedance stability was controlled using a rectangular transition step with appropriate dimensions. The patch radiator for the entire bandwidth and the ground plane are significantly influenced by these dimensions. A double-slant feeder technique is used to control the matching between the patch and its feeder. Also, it has been concluded that the changing of these triangular shapes has a considerable influence on the higher frequencies of the operational bandwidth. The results show that a 24% reduction in the first resonant frequency was observed when an L-shaped slot was used in comparison with that without a slot. Based on this, a 38% reduction in the size of the antenna can be obtained. In summary, in addition to an enhanced antenna gain and a wider impedance bandwidth when the proposed antenna is used, the reduction in resonant frequency also leads to a possible reduction in the size of the antenna. All of these merits are considered advantages over compact designs with a slotted radiating patch. For indoor wireless communication applications, such merits are considered advantageous.

REFERENCES

[1] Hasan, Y. M., A. S. Abdullah, and F. M. Alnahwi, "Dual-port filtenna system for interweave cognitive radio applications," *Ira-*

nian Journal of Science and Technology, Transactions of Electrical Engineering, Vol. 46, No. 4, 943–958, 2022.

[2] FCC, "First report and order on ultra-wideband technology," Washington, DC, USA, 2002.

[3] Panda, J. R., P. Kakumanu, and R. S. Kshetrimayum, "A wideband monopole antenna in combination with a UWB microwave band-pass filter for application in UWB communication system," in *2010 Annual IEEE India Conference (INDICON)*, 1–4, Kolkata, India, 2010.

[4] Win, M. Z., D. Dardari, A. F. Molisch, W. Wiesbeck, and J. Zhang, "History and applications of UWB," in *Proceedings of the IEEE*, Vol. 97, No. 2, 198–204, 2009.

[5] Kumar, O. P., P. Kumar, T. Ali, P. Kumar, and S. Vincent, "Ultrawideband antennas: Growth and evolution," *Micromachines*, Vol. 13, No. 1, 60, 2021.

[6] Abbas, A., N. Hussain, M. A. Sufian, J. Jung, S. M. Park, and N. Kim, "Isolation and gain improvement of a rectangular notch UWB-MIMO antenna," *Sensors*, Vol. 22, No. 4, 1460, 2022.

[7] Khan, M. S., S. A. Naqvi, A. Iftikhar, S. M. Asif, A. Fida, and R. M. Shubair, "A WLAN band-notched compact four element UWB MIMO antenna," *International Journal of RF and Microwave Computer-Aided Engineering*, Vol. 30, No. 9, e22282, 2020.

[8] Perli, B. R. and M. R. Avula, "Design of wideband elliptical ring monopole antenna using characteristic mode analysis," *Journal of Electromagnetic Engineering and Science*, Vol. 21, No. 4, 299–306, 2021.

[9] Abbas, A., N. Hussain, M.-J. Jeong, J. Park, K. S. Shin, T. Kim, and N. Kim, "A rectangular notch-band UWB antenna with controllable notched bandwidth and centre frequency," *Sensors*, Vol. 20, No. 3, 777, 2020.

[10] Rizvi, S. N. R., W. A. Awan, D. Choi, N. Hussain, S. G. Park, and N. Kim, "A compact size antenna for extended UWB with WLAN notch band stub," *Applied Sciences*, Vol. 13, No. 7, 4271, 2023.

[11] Sandu, D. D., O. Avadanei, A. Ioachim, G. Banciu, and P. Gasner, "Microstrip patch antenna with dielectric substrate," *Journal of Optoelectronics and Advanced Materials*, Vol. 5, No. 5, 1381–1387, 2003.

[12] Kumar, P. C. P. and P. T. Rao, "Dual staircase shaped microstrip patch antenna," in *2015 International Conference on Pervasive Computing (ICPC)*, 1–5, Pune, India, 2015.

[13] Yeom, I., Y. B. Jung, and C. W. Jung, "Wide and dual-band MIMO antenna with omnidirectional and directional radiation patterns for indoor access points," *Journal of Electromagnetic Engineering and Science*, Vol. 19, No. 1, 20–30, 2019.

[14] Tangwachirapan, S., W. Thaiwirot, and P. Akkaraekthalin, "Design and analysis of antipodal vivaldi antennas for breast cancer detection," *Computers, Materials & Continua*, Vol. 73, No. 1, 411–431, 2022.

[15] Al-Gburi, A., I. B. M. Ibrahim, Z. Zakaria, B. H. Ahmad, N. Shairi, and M. Y. Zeain, "High gain of UWB planar antenna utilising FSS reflector for UWB applications," *Computers, Materials & Continua*, Vol. 70, No. 1, 1425–1436, 2022.

[16] Muzaffar, S., D. Turab, M. Zahid, and Y. Amin, "Dual-band UWB monopole antenna for IoT applications," *Engineering Proceedings*, Vol. 46, No. 1, 29, 2023.

[17] Sakshi, and M. Bharti, "Penta-band planar monopole circular antenna design using inverted L-shaped slot for UWB application," *Journal of Electronic Materials*, Vol. 52, No. 12, 8281–8292, 2023.

[18] Hasan, Y. M., A. S. Abdullah, and F. M. Alnahwi, "UWB filtenna with reconfigurable and sharp dual-band notches for underlay cognitive radio applications," *Progress In Electromagnetics Research C*, Vol. 120, 45–60, 2022.

[19] Sambandam, P., M. Kanagasabai, R. Natarajan, M. G. N. Alsath, and S. Palaniswamy, "Miniaturized button-like WBAN antenna for off-body communication," *IEEE Transactions on Antennas and Propagation*, Vol. 68, No. 7, 5228–5235, 2020.

[20] Yang, W., Y. Zhang, W. Che, M. Xun, Q. Xue, G. Shen, and W. Feng, "A simple, compact filtering patch antenna based on mode analysis with wide out-of-band suppression," *IEEE Transactions on Antennas and Propagation*, Vol. 67, No. 10, 6244–6253, 2019.

[21] Liao, C., L. Zhang, G. Zhang, C. Lu, and X. Zhang, "Partial discharge wideband full-band high-gain resonant cavity UHF sensor research," *Sensors*, Vol. 23, No. 15, 6847, 2023.

[22] Benkhadda, O., S. Ahmad, M. Saih, K. Chaji, A. Reha, A. Ghaffar, S. Khan, M. Alibakhshikenari, and E. Limiti, "Compact broadband antenna with vicsek fractal slots for WLAN and WiMAX applications," *Applied Sciences*, Vol. 12, No. 3, 1142, 2022.

[23] Balanis, C. A., *Antenna Theory: Analysis and Design*, John Wiley & Sons, 2015.

[24] Martínez-Lozano, A., C. Blanco-Angulo, H. García-Martínez, R. Gutiérrez-Mazón, G. Torregrosa-Penalva, E. Ávila Navarro, and J. M. Sabater-Navarro, "UWB-printed rectangular-based monopole antenna for biological tissue analysis," *Electronics*, Vol. 10, No. 3, 304, 2021.

[25] Hasan, Y. M., A. S. Abdullah, and F. Alnahwi, "Three-modes, reconfigurable filtenna system with UWB, WiMAX, and WLAN states for cognitive radio applications," *International Journal on Communications Antenna and Propagation (IRECAP)*, Vol. 14, No. 1, 15–23, 2024.

[26] Saeidi, T., I. Ismail, W. P. Wen, A. R. H. Alhawari, and A. Mohammadi, "Ultra-wideband antennas for wireless communication applications," *International Journal of Antennas and Propagation*, Vol. 2019, No. 1, 7918765, 2019.

[27] Xu, G., V. G. Ataloglou, S. V. Hum, and G. V. Eleftheriades, "Extreme beam-forming with impedance metasurfaces featuring embedded sources and auxiliary surface wave optimization," *IEEE Access*, Vol. 10, 28 670–28 684, 2022.

[28] Liu, L., Y. Yang, C. Yu, S. Li, H. Wu, L. Sun, and F. Meng, "A substrate integrated waveguide-based w-band antenna for microwave power transmission," *Micromachines*, Vol. 13, No. 7, 986, 2022.

[29] Hasan, Y. M., K. D. Rahi, and A. A. Mahmood, "Rectangular antenna with dual-notch band characteristics for UWB applications," in *AIP Conference Proceedings*, Vol. 2591, No. 1, 020032, AIP Publishing, 2023.

[30] Saini, R. K., S. Dwari, and M. K. Mandal, "CPW-fed dual-band dual-sense circularly polarized monopole antenna," *IEEE Antennas and Wireless Propagation Letters*, Vol. 16, 2497–2500, 2017.

[31] Sediq, H. T., J. Nourinia, C. Ghobadi, and B. Mohammadi, "A novel shaped ultrawideband fractal antenna for medical purposes," *Biomedical Signal Processing and Control*, Vol. 80, 104363, 2023.

[32] Wang, M., H. Wang, P. Chen, T. Ding, J. Xiao, and L. Zhang, "A butterfly-like slot UWB antenna with WLAN band-notch characteristics for MIMO applications," *IEICE Electronics Express*, Vol. 19, No. 14, 20 220 233–20 220 233, 2022.

[33] Saha, T. K., C. Goodbody, T. Karacolak, and P. K. Sekhar, "A compact monopole antenna for ultra-wideband applications," *Microwave and Optical Technology Letters*, Vol. 61, No. 1, 182–186, 2019.